HHS Public Access

Author manuscript

Pharm Res. Author manuscript; available in PMC 2023 October 09.

Published in final edited form as:

Pharm Res. 2022 December ; 39(12): 3317–3330. doi:10.1007/s11095-022-03409-5.

Development of a High-Dose Infant Air-Jet Dry Powder Inhaler (DPI) with Passive Cyclic Loading of the Formulation

Connor Howe[1], **Mohammad A.M. Momin**[2], **Ghali Aladwani**[1], **Michael Hindle**[2], **Worth Longest**[1,2,*]

[1]Department of Mechanical and Nuclear Engineering, Virginia Commonwealth University, Richmond, VA

[2]Department of Pharmaceutics, Virginia Commonwealth University, Richmond, VA

Abstract

Purpose—The objective of this study was to incorporate a passive cyclic loading strategy into the infant air-jet dry powder inhaler (DPI) in a manner that provides high efficiency aerosol lung delivery and is insensitive to powder mass loadings and the presence of downstream pulmonary mechanics.

Methods—Four unique air-jet DPIs were initially compared and the best performing passive design (PD) was selected for sensitivity analyses. A single preterm *in vitro* nose-throat (NT) model, air source, and nasal interface were utilized throughout. While the majority of analyses were evaluated with a model spray-dried excipient enhanced growth (EEG) formulation, performance of a Surfactant-EEG formulation was also explored for the lead DPI design.

Results—Two devices, PD-2 and PD-3, evaluated in the preterm model achieved an estimated lung delivery efficiency of 60% with the model EEG formulation, and were not sensitive to the loaded dose (10-30 mg of powder). The PD-3 device was also unaffected by the presence of downstream pulmonary mechanics (infant lung model) and had only a minor sensitivity to tripling the volume of the powder reservoir. When using the Surfactant-EEG formulation, increasing the actuation flow rate from 1.7 to 4.0 L/min improved lung delivery by nearly 10%.

Conclusions—The infant air-jet DPI platform was successfully modified with a passive cyclic loading strategy and capable of providing an estimated >60% lung delivery efficiency of a model spray-dried formulation with negligible sensitivity to powder mass loading in the range of 10-30 mg and could be scaled to deliver much higher doses.

[*]**Corresponding Author Contact Information:** P. Worth Longest, PhD, Virginia Commonwealth University, 401 West Main Street, P.O. Box 843015, Richmond, VA 23284-3015, Phone: (804)-827-7023, Fax: (804)-827-7030, pwlongest@vcu.edu.
Connor Howe, BS, *Affiliation and Address:* Virginia Commonwealth University, 401 W Main Street, PO Box 843015, Richmond, VA 23284, howec@vcu.edu
Michael Hindle, PhD, *Affiliation and Address:* Virginia Commonwealth University, 410 N. 12th Street, PO Box 980533, Richmond, VA 23284, mhindle@vcu.edu
Ghali Aladwani, MS, *Affiliation and Address:* Virginia Commonwealth University, 401 W Main Street, PO Box 843015, Richmond, VA 23284, aladwanigh@vcu.edu
Mohammad A.M. Momin, PhD, *Affiliation and Address:* Virginia Commonwealth University, 410 N. 12th Street, PO Box 980533, Richmond, VA 23284, mammomin@vcu.edu

AUTHOR DISCLOSURE STATEMENT

Virginia Commonwealth University is currently pursuing patent protection of devices and methods described in this study, which if licensed and commercialized, may provide a future financial interest to the authors.

Keywords

Trans-nasal aerosol delivery; nose-to-lung aerosol delivery; infant DPI; inline DPI; passive cyclic loading

INTRODUCTION

Challenges associated with pharmaceutical aerosol delivery to infants include poor lung delivery efficiency, high intersubject dose variability and long administration times (1-5). For example, in the *in vivo* study of Fok et al. (6), a group of 13 spontaneously breathing infants received radio-labelled salbutamol delivered through a metered dose inhaler (MDI) with a valved holding chamber and facemask. With two actuations of the MDI, the mean lung dose was 1.35 μg across the population, with lung delivery efficiencies to all infants <2.5% of the loaded dose. Perhaps even more concerning than poor lung delivery efficiency is high intersubject variability, where in the study of Fok et al. (6) one infant received a lung dose of only 0.25 μg and another received 4.52 μg, indicating the dose received may be approximately 5-fold lower or 3-fold higher than the mean of 1.35 μg. A more recent example of poor infant lung delivery efficiency is the *in vivo* study of Corcoran et al. (7), in which a radiopharmaceutical aerosol was administered to 18 infants via mesh nebulizer through a nasal cannula interface while simultaneously receiving nasal cannula oxygen. It was estimated that only 0.46% of the nebulized dose reached the lungs at a cannula flow rate of 2 L/min, with an overall high variability in delivered dose. These findings are consistent with most other *in vivo* and realistic *in vitro* infant studies, resulting in lung delivery efficiency values in the range of 0-10% of the loaded or nebulized dose (8-15) across multiple inhalation platforms. These low lung delivery efficiencies combined with high intersubject variabilities can often result in extended treatment times, poor clinical response and elevated off-target effects, especially when administering medications that require relatively high lung doses or that have a narrow therapeutic window.

To better address the challenges associated with pharmaceutical aerosol delivery to infants, our group (16-18) is developing an infant air-jet dry powder inhaler (DPI) platform. Overall, the infant air-jet DPI is designed to provide a full inhalation breath along with the aerosol to the lungs of an infant through the nasal route. The platform consists of an air source (providing aerosolization energy and inhalation breath), the air-jet DPI (responsible for holding and aerosolizing the loaded powder), and the nasal interface, which transports the aerosol from the DPI to the infant's nasal passage and forms an airtight seal with the infants nostrils. Previous studies of the infant air-jet DPI have evaluated the effects of the aerosolization chamber geometry (16), air source and flow rate (17), and infant nasal interfaces (18). Overall, the best performing configuration of the infant air-jet DPI platform was able to deliver ~57% of the loaded dose to the tracheal filter through an *in vitro* preterm NT model (18); however, this configuration held only ~10-20 mg of the dry powder formulation before needing to be reloaded.

The infant air-jet DPI is viewed as a general aerosol delivery platform with multiple potential applications. These potential uses of the platform where high efficiency lung

delivery of a pharmaceutical aerosol may be beneficial include administering inhaled surfactant in surfactant replacement therapy (19, 20), inhaled antibiotics to treat bacterial pneumonia (21), and inhaled antivirals to treat RSV and severe viral pneumonia (22, 23). In each of these envisioned applications, relatively high doses of powder, typically in the range of 10 mg and above for an infant, are expected to be required to generate a sufficient biological response. Even in adults, the availability of high dose DPIs is limited, with some newer devices administering >10 mg of drug (24-27). However, these devices are designed to operate with very large inhaled air volumes (on the order of ~2 L and above), high airflow rates (typically 45 L/min and above), and may incur significant extrathoracic depositional losses. Alternatively, higher dose delivery is often accomplished by requiring the patient to use a relatively low dose device and load multiple capsules with repeated inhalations over multiple cycles (28, 29), which increases the difficulty of device operation as well as the opportunity for user errors (30). Ideally, a general high dose DPI platform should allow for different powder mass loadings without significantly impacting performance or operation, and will likely require multiple breaths to maintain an acceptable lung deposited powder mass with each inhalation. Considering the infant air-jet DPI applied to high dose applications, what is needed is a system that will enable increased powder mass loadings without impacting the previously achieved high lung delivery efficiency.

Options to increase the aerosolized dose of the infant air-jet DPI include (i) use of a larger aerosolization chamber to accommodate more loaded powder or (ii) development of a cyclic loading strategy that is employed automatically by the device. Preliminary experiments have indicated that increasing the infant air-jet DPI aerosolization chamber volume to accommodate higher mass loadings negatively impacts aerosol performance (with current chamber designs) especially when only 10 mL of air is available to aerosolize the powder. Furthermore, repeated exposure of dry powder formulations to aerosolization forces within the device creates aggregates that are then difficult to disperse with subsequent actuations. As an alternative to simply increasing the aerosolization chamber volume, we propose a *passive cyclic loading strategy* that employs separate powder reservoir and aerosolization chamber components. Variable powder doses may be loaded into the powder reservoir, which connects to the aerosolization chamber. This enables the aerosolization chamber to maintain previously established dimensions and flow conditions that have been shown to be conducive for high efficiency aerosolization (16-18). A combination of the connection design leading from the reservoir and a potential metering system may control the dose loaded into the aerosolization chamber that is then converted to an aerosol with each actuation.

With a passive cyclic loading strategy, introduction of a *metering element*, such as a *powder tray*, may be used to further control the amount of powder that is aerosolized with each actuation. Goals of the passive cyclic loading system include metering a consistent amount of powder for each actuation while protecting the powder in the reservoir from aggregate formation. If designed properly, the result should be a single device that can accommodate a variable range of powder doses and aerosolize a relatively consistent amount of dose with each actuation, while remaining insensitive to the amount of powder loaded (above a certain threshold). Accomplishing this goal with forces already present in the device and very small volumes of actuation air presents a significant challenge for infant aerosol delivery.

The objective of this study was to expand the infant air-jet DPI with a passive cyclic loading strategy that provides high efficiency lung delivery of an aerosol and is insensitive to powder mass loadings in the range of 10-30 mg as well as the presence of downstream pulmonary mechanics. As a secondary objective, this study will also explore the impact of different powder reservoir sizes, formulation types and actuation gas flow rates on performance of the new device. The study begins by comparing four new air-jet DPIs with a passive cyclic loading design using the initial 10 mg powder mass. The best designs (based on highest tracheal filter deposition percentage, which estimates the lung delivery efficiency) are then loaded with a 30 mg powder mass and performance is re-examined. The goal of the new designs is to produce similar aerosolization performance and lung delivery efficiencies independent of the loaded powder mass (10 vs 30 mg). A secondary goal is to improve upon our previous best performing infant air-jet DPI platform configuration by reaching a lung delivery efficiency of 60% using a highly dispersible spray-dried model excipient enhanced growth (EEG) formulation and realistic preterm nose-throat model. Next, a single design is chosen for continued sensitivity analysis including downstream pulmonary mechanics and powder reservoir volume size (the initial standard vs an extended volume size). Finally, the performance of the platform with a spray-dried Surfactant-EEG formulation (20) is investigated, as well as a re-examination of the effect of flow rate.

MATERIALS AND METHODS

Powder Materials and Formulation

Albuterol sulfate (AS) and l-leucine were purchased from Sigma Chemical Co. (St. Louis, MO). Pearlitol® PF-Mannitol was donated from Roquette Pharma (Lestrem, France) and Poloxamer 188 (Leutrol F68) was donated from BASF Corporation (Florham Park, NJ). Trileucine was purchased from Bachem Americas, Inc. (Torrance, CA). Sodium chloride, ethanol and methanol were purchased from Fisher Scientific Co. (Hanover Park, IL). Survanta® (beractant) intratracheal suspension was purchased from Cardinal Health, Inc. (Greensboro, NC). Throughout the study, freshly collected deionized water was used.

A batch of AS excipient enhanced growth (AS-EEG) powder was obtained using a Büchi Nano B-90 HP Spray Dryer (Büchi Laboratory-Techniques, Flawil, Switzerland), and spray-dried based on the optimized method described by Son et al. (31). The AS-EEG powder formulation included 30:48:20:2% w/w ratio of AS, mannitol, trileucine, and Poloxamer 188, respectively. A feed solution of 150 mL containing the dissolved drug and excipients at the stated ratio was sprayed over a 4 hour period at a spray rate of 0.6 mL/min. The solids concentration in the feed solution was 0.5% w/v. Throughout the spray drying process, the inlet temperature was set to 120 °C, resulting in an outlet temperature of 49 °C. The feed solution reservoir was placed in a thermostat-controlled chiller and its temperature was maintained at 5-15 °C during the spray drying. Excess solution delivered to the spray head by a peristatic pump that was not sprayed was recirculated via an outlet tube and returned to the feed solution reservoir.

Two batches of Survanta® based Surfactant-EEG powders were prepared by spray drying of the feed dispersions containing Survanta®, mannitol, sodium chloride and l-leucine at a ratio of 40:30:10:20% w/w using the Buchi Nano Spray Dryer B-90 HP (Büchi Labortechnik

AG, Flawil, Switzerland). The feed dispersions were prepared with 0.125% w/v solids by addition of all the formulation components to 5% v/v ethanol in water followed by 40 min sonication in a heated water bath (Fisher Scientific™ CPXH, Hanover Park, IL) at 45-55°C. The prepared feed dispersions were spray-dried with the spray dryer in an open mode configuration using the small nozzle and the following optimized operating conditions reported by Boc et al. (32). Throughout the spray drying process, the inlet temperature was set to 70 °C, resulting in an outlet temperature of 35-38 °C. The spray-dried powders were collected from the electrostatic precipitator into glass vials and stored in a desiccator (0% RH) in the freezer (−20 °C) when not in use.

Infant Air-Jet Platform and Experimental Overview

The infant air-jet DPI platform (16-18) is comprised of three main components: the air source, the air-jet DPI, and the nasal interface (Fig. 1). The air source is responsible for providing the aerosolization energy to the air-jet DPI, as well as delivering the aerosolized powder to the lungs while providing a full inhalation breath for the infant. For all experiments, the electronic *Timer* air source was utilized as developed and described by Howe et al. (17). The air source at baseline conditions delivers an air actuation volume (AAV) of 10 mL bursts at a Q90 flow rate of 1.7 L/min. For each trial, a neonatal mass flow meter (Sensirion SFM3400, Sensirion AG, Stafa, Switzerland) was used to calibrate and verify the air source actuation parameters. Figure 1 shows the location of the mass flow meter connected between the air source and air-jet DPI. The air-jet DPI consists of small diameter flow pathways for the inlets and outlets connected by an aerosolization chamber (Figure 2) and is responsible for aerosolization of the powder as well as holding the full dose of powder. In this study, as the air source is actuated, high speed jets of air pass through the aerosolization chamber and either around or through the preloaded powder facilitating powder aerosolization and a passive cyclic loading action. Four unique air-jet DPI designs (Figure 2) were developed and are described in more detail in the “Air-Jet DPI Designs” subsection. After exiting the air-jet DPI, the formed aerosol then passes through the nasal interface and to the infant (Figure 1). The prong of the nasal interface is inserted approximately 5 mm into the nose, consistent with short ventilation support nasal prongs and forms an airtight seal with the nostril.

A single nasal interface was used for all experiments in this study consisting of a gradually expanding flow pathway and rigid curved prong (Figure 3) based on results of previous nasal interface testing (18). Slight modifications were made to the nasal interface based on additional testing. The nasal interface in this study consisted of a straight gradually expanding circular cross-section with a length of 48 mm, and a final internal diameter of 3.6 mm. The end of the expansion transitioned to a rigid curved prong (Figure 3), with an inner diameter of 3.6 mm and outer diameter of 4.6 mm. The outer diameter of the prong was based on a Hudson Prong Size 2, commonly used for preterm infant nasal continuous positive airway pressure (CPAP) administration. A gradual exterior taper was included at the base of the prong, forming a wedge to help facilitate an airtight seal with the infant’s nostril (Figure 3). The nasal interface was built using stereo-lithography (SLA) with Accura ClearVue resin through 3D Systems On Demand Manufacturing.

The main portion of this study compares the different air-jet DPI designs using a preterm infant nose-throat (NT) *in vitro* model and a 10 mg loaded powder mass of AS-EEG formulation. As seen in Figure 1, the platform interfaces with the preterm NT model which leads to a custom low-volume filter for approximating lung delivered dose. In this setup, device ED, nasal interface deposition, NT regional depositions, and lung delivery efficiency (represented by aerosol passing through the larynx and a portion of the trachea and depositing on the filter) were assessed, as percentage values of the loaded dose. The best performing devices were then selected for dose loading sensitivity in which a 30 mg loaded powder mass was also tested. A pulmonary mechanics sensitivity comparison was also performed to test the performance of the platform while connected to an infant lung simulator that provided realistic downstream resistance and compliance. To enable larger mass loadings for high dose applications or lower density powder formulations, a loading chamber volume sensitivity experiment was also performed. As a final step, this study explored the use of a Surfactant-EEG formulation in the best performing device. Sensitivity of the platform to powder formulation was explored as well as the effect of flow rate on the new formulation.

Preterm Infant Nose-Throat (NT) Model

For all experiments in this study, a previously developed (17, 18) preterm NT *in vitro* model was used. The scaled 6-month preterm NT airway model includes flexible nostrils and anterior nose connected to a rigid middle passage, throat and approximately 3/4th of the trachea, which then connects to a custom low-volume filter housing. Figure 4a illustrates the setup and assembly break-out of the NT model and low-volume filter housing. Briefly, the preterm infant airway geometries were scaled down to an infant with a weight of 1600 g and length (height) of 40.7 cm, based on a high-quality CT scan of 6-month-old infant NT geometry (33). Using the infant body length (height), an appropriate geometric scaling factor of 0.6 was applied to the 6-month-old NT airway to reduce the model to that of a preterm infant with weight and height of about 1600 g and 40.7 cm, respectively (34). The resulting preterm airway, shown in Figure 4b, has a tracheal length and diameter (proximal) of approximately 26 and 3 mm, respectively. While these parameters are known to vary, they do fall within the expected range for preterm infants of 25 to 30 weeks gestational age (GA) based on reported studies (35).

The scaled 6-month preterm NT model was constructed with twist lock interfaces and O-rings that provided air tight seals and facilitated ease of use. The low-volume filter housing accommodated the low AAV of 10 mL used for a preterm infant, with a dead space of only 2.7 mL before the 1.5” diameter glass-fiber filter. To provide a smooth and accurate internal airway surface, the middle passage and throat sections of the preterm NT model were built using SLA printing with Accura ClearVue resin (3D Systems). The low-volume filter housing was 3D printed using VeroWhitePlus resin. To facilitate nasal interface prong insertion and the formation of an airtight seal, the face and anterior nose section were molded with a skin-like silicone elastomer. The face adapter (pictured in Figure 4a) was printed using VeroWhitePlus resin, and was glued to the soft face mold, allowing for a secure and air-tight connection to the rest of the NT model. The three distinct airway regions

of the NT model used for regional deposition quantification (anterior nose, middle passage, and throat) are illustrated in Figure 4b.

Air-Jet DPI Designs

Four unique air-jet DPIs were designed and prototyped to investigate passive cyclic loading for the platform. Figure 2 shows the internal airway geometries of each air-jet DPI passive design (PD), labeled as PD-1 through PD-4, with basic elements including small diameter inlet flow passage(s), aerosolization chamber, powder reservoir (where the powder was initially loaded), and outlet capillary. In each design, the powder reservoir was positioned above (with respect to gravity) the aerosolization chamber, centered perpendicular to the direction of primary air flow. In this study, the powder reservoir was filled with the desired dose (mass of powder) and then connected to the air-jet DPI with a twist-lock and O-ring seal. The initial standard powder reservoir could accommodate a powder volume up to 0.55 mL. Each air-jet PD had identical connections for powder reservoir attachment, while the inlets, aerosolization chamber geometries, and outlets differed. Several rounds of preliminary screening were performed for each of the four designs in this study leading to a relative best case for each PD geometry. For the initial comparison of the four unique air-jet DPI designs, the number of actuations to clear the device was also recorded, in which actuations continued until two consecutive visibly clear (no aerosol visible passing through the nasal interface) actuations were observed. This metric helped to distinguish future ease of use and speed of delivery, with a lower number of actuations indicating quicker delivery times to administer a full dose.

All designs were influenced by our previous studies with modifications made to explore passive cyclic loading. As with previous infant air-jet DPIs, the four new designs in this study (Figure 2a-d) all used a single outlet capillary from the aerosolization chamber (inner diameter of 0.89 mm and a flush or protruding configuration) comprised of a hollow stainless steel (SAE 304) capillary tube. After exiting the aerosolization chamber, this capillary tube included a 37 degree downward bend prior to connection with the nasal interface. All devices used a flush (capillary does not protrude into the aerosolization chamber) outlet configuration with the exception of PD-3, in which the capillary tube protruded into the aerosolization chamber by 0.5 mm. PD-1 and PD-4 used a single inlet of 0.6 mm diameter while PD-2 and PD-3 used multiple inlets with 0.5 mm diameters. These inlet geometries were formed into the structure of the air-jet device during 3D printing. One subtle difference in inlet configurations was that PD-2 had four inlets, all directing the inlet airflow around the initial powder bed. PD-3 had three inlets with one directing a portion of the inlet flow toward the powder bed and the other two directing the airflow through the lower region of the aerosolization chamber.

Considering the aerosolization chambers, PD-1 included a small spherical geometry (diameter of 4.8 mm) with a 3 mm diameter connection to the powder reservoir. PD-2 and PD-3 both had a horizontal capsule shaped aerosolization chamber with a volume ~0.68 mL, and a powder shelf or tray placed directly below the powder reservoir to facilitate dose metering. The PD-2 device used a 3 mm diameter opening to the powder reservoir with the shelf positioned to provide an approximate 0.026 mL volume for the powder to rest during

each actuation. The PD-3 device used a 2.7 mm diameter opening to the powder reservoir with the shelf positioned to provide an approximate 0.013 mL volume for powder metering. PD-4 used a small aerosolization chamber of ~0.05 mL with two small (1 mm diameter) openings to the powder reservoir, spaced equidistance between the inlet/outlet and center of the chamber (as pictured in Figure 2d).

All air-jet DPI parts (as well as nasal interface and NT model parts) were designed in SolidWorks (Dassault Systèmes, Paris, France), and exported as .STL files. The parts were then 3D printed at either 32 μm resolution on a Stratasys Objet24 3D Printer (Stratasys Ltd., Eden Prairie, MN) using VeroWhitePlus resin, or with stereo-lithography (SLA) using Accura ClearVue resin through 3D Systems On Demand Manufacturing with a layer thickness of 0.05 mm. All parts were designed to interconnect using a twist lock mechanism with an intermediate O-ring for an air-tight seal.

In Vitro Evaluation of Preterm Lung Delivery Efficiency

To assess the aerosol transmission through the nose and throat, and effective lung delivery efficiency (drug deposited on the filter), all experiments utilized the scaled 6-month preterm NT *in vitro* model. The nasal interface, as seen in Figure 3, was inserted approximately 5 mm into the left nostril of the infant NT model while the right nostril was manually held closed during actuation. A small amount of lubricant grease was applied to the exterior of the prong to ensure an airtight seal. The internal airways of all NT model segments were coated with a silicon spray to minimize particle bounce and simulate airway surface liquid. At the end of the NT model, a custom low-volume filter collected powder passing through the extrathoracic regions and represented the amount of drug delivered to the lung. Calculations for ED and regional depositions, including the nasal interface and in the NT model regions and tracheal filter, were expressed as a percentage of the manually weighed loaded dose of AS. All experiments were performed in triplicate for the calculation of mean and standard deviation values. More detail on the regional deposition fractions can be found in the “Drug Mass Characterization Methods” subsection.

Sensitivity Analysis

Impact of Loaded Dose—To determine potential sensitivity to powder loading between the initial mass of 10 mg and a larger mass of 30 mg, additional experiments were performed for the two best case designs (PD-2 and PD-3), in which a 30 mg powder mass loading was used. All experimental procedures remained the same as with the air-jet DPI comparison set, except for the manual weighing of 30 mg of powder instead of 10 mg. Likewise, actuations continued until no powder was visible passing through the system and one subsequent clear actuation was performed. The total number of actuations used in all cases was recorded.

Impact of Downstream Pulmonary Mechanics—To test sensitivity of the platform to downstream pulmonary mechanics, the PD-3 air-jet DPI design was chosen and retested while connected to an infant Michigan Lung simulator (Adult/Infant Model, Michigan Instruments, Grand Rapids, MI). Two NT model outlet conditions were considered: one as the standard filter only (used in all other experiments) and then also including the

downstream pulmonary mechanics, connected to the lung simulator. This experiment was performed to directly compare the large dose loading condition including downstream pulmonary mechanics in a breathing lung simulator, as pictured in Figure 5. Using the air source operated at 1.7 L/min, and a 30 mg powder mass loading, the platform was actuated during the inhalation cycle of the lung simulator, while all other methods remained the same. Pulmonary mechanics (PM) considered in this study were lung compliance (mL/cm H_2O), airway resistance (cm H_2O/L/s), breath cycle (sec), and tidal volume (mL). The compliance, breath cycle, and tidal volume were manually set on the lung simulator, and a custom resistance orifice adapter was used to adjust the airway resistance.

While values for these properties are known to vary, our previous study examining pulmonary mechanics (17) used a compliance of 0.49 mL/cm H_2O for a 1600 g preterm infant based on similar values measured in infants with a weight of 1600 g (36). For this study, the infant lung simulator was set to its lowest compliance setting of 1 mL/cm H_2O. The inspiratory time was set to 0.5 sec, with a 1 sec breath hold and exhalation period resulting in a ~2.5 sec breath cycle. With the direct-to-infant delivery protocol used in this study, one nostril was connected to the device while the contralateral nostril and mouth were held closed enabling the use of a breath hold period. The tidal volume was adjusted to approximately 10-11 mL. For infants with RDS, airway resistance values have been reported between 100-200 cm H_2O/L/s (36-39). An adjustable resistance orifice was built to set the desired airway resistance downstream of the filter. To measure airway resistance through the filter housing and orifice, a pressure sensor (SSCDLNN040MBGSA5, Honeywell, Sensing and Control, Golden Valley, MN) was placed anterior to the filter housing while the neonatal flow meter (Sensirion SFM3400) was placed further upstream. The downstream side of the resistance orifice was opened to atmospheric pressure while a steady upstream flow rate of 2 L/min was set. The pressure was recorded while the orifice was adjusted to provide a total airway resistance expected for an infant with RDS. The resulting calculated resistance was 172 cm H_2O/L/s which falls within the range of expected values.

As with our previous study including pulmonary mechanics (17), air flow from exhalation of the lung simulator was prevented from passing back through the filter and detaching any deposited powder. The use of one-way valves and a bifurcation downstream of the resistance orifice allowed for venting the exhalation gas, as seen in Figure 5.

Impact of Powder Reservoir Volume—To enable larger dose loadings of powder, an extended powder reservoir was also considered. Both powder reservoirs had similar geometry with a half capsule shape of 7.1 mm diameter, differing by length only. The standard powder reservoir had a loading volume of 0.55 mL, while the extended volume was 1.5 mL, and both reservoirs were fabricated using the SLA method to produce clear parts for viewing of powder behavior during actuation. Images of the two translucent powder reservoirs connected to the opaque PD-3 device can be seen in Figure 6. The standard powder reservoir could accommodate dose loadings between 10-50 mg of the AS-EEG formulation used in this study, which had a bulk density of ~0.1 g/cm^3 and up to ~150 mg with the extended version. For this experiment, PD-3 was chosen with a 10 mg powder mass loading, while all other parameters remained the same as the initial experimental set.

Impact of Surfactant Formulation—Different dry powder formulations containing specific active pharmaceutical ingredients for a target disease state are expected to have different properties and different aerosolization characteristics. For this study, the Surfactant-EEG formulation was chosen for comparison with the model AS-EEG formulation. The PD-3 design was chosen for formulation sensitivity of the platform using a 10 mg mass loading of Surfactant-EEG. All other experimental parameters remained the same.

Impact of Surfactant Formulation Across Different Flow Rates—As mentioned in the previous air source study (17), the ideal flow rate is likely device and/or formulation dependent. While a Q90 flow rate of 1.7 L/min was ideal for dispersion and delivery of the AS-EEG formulation, it may not be ideal for the case of Surfactant-EEG. Two additional flow rates (i.e., 4 and 6 L/min) were chosen to compare aerosol delivery performance with the PD-3 device and the Surfactant-EEG formulation. To generate these flow rates, the Timer air source was adjusted to 0.15 and 0.1 second delivery times, respectively, which maintained the ~10 mL AAV in each case.

Drug Mass Characterization Methods

For the AS-EEG formulation, after approximately 4 to 8 actuation cycles, drug masses retained or deposited on the air-jet DPI, nasal interface, NT model, and filter were recovered by dissolving in an appropriate volume of deionized water followed by high performance liquid chromatography (HPLC) analysis with fluorescence detection (excitation = 276 nm, emission = 609 nm). A Restek Allure PFP propyl column (5 μm, 60 Å, 150 x 2.1 mm) was used for the chromatographic separation with a mobile phase flow rate of 0.4 mL/min. The mobile phase consisted of methanol and ammonium formate buffer (20 mM, pH 3.4 through addition of formic acid) in a ratio of 70:30, and the sample injection volume was 10 μL. The loaded drug mass was determined through content uniformity analysis of the AS-EEG formulation; where known masses of AS-EEG were dissolved in water and the AS content (μg/mg of formulation) was determined. AS quantification was performed for each deposition site and for the total drug mass used to calculate the drug recovery. Drug recovery percentages were expressed as the sum of the amount of AS recovered in each deposition region divided by the loaded AS dose for each experiment. The calibration curve was linear ($R^2 > 0.995$) over the concentration range of 0.5–20 μg/mL. The limit of detection (LOD) and limit of quantitation (LOQ) were 0.06 and 0.17 μg/mL, respectively. The accuracy (as %bias) at concentrations of 5, 10 and 15 μg/mL was ≤5% and precision (as %RSD) was ≤2%.

For the Surfactant-EEG formulation, the surfactant content was determined based on the content of dipalmitoylphosphatidylcholine (DPPC). The DPPC content was quantified using a liquid chromatography–mass spectrometry (LC-MS) method adapted from Li et al. (40). The system consisted of the Quattro micro™ mass spectrometer linked to an Alliance 2695 Separations Module with data acquisition software, MassLynx v4.1 (all from Waters Corporation, Milford, MA). The chromatographic separation was achieved using the Atlantis hydrophilic interaction liquid chromatography (HILIC) silica column (5 μm, 50×1.0 mm; Waters Corporation, Milford, MA). The isocratic mobile phase consisted of acetonitrile and 5 mM ammonium formate in water with 0.1% formic acid (88:12% v/v) pumped at a

flow rate of 0.3 mL/min. The injection volume was 10 μL. Following optimization of the ionization settings of the mass spectrometer, selected ion monitoring (SIM) analysis (for m/z = 735) with positive electrospray ionization mode was applied to detect and quantify DPPC (molecular weight = 734 Daltons) following chromatographic separation. The DPPC stock standard solution (20 μg/mL) was prepared by dissolving sufficient amount of DPPC (Avanti Polar Lipids, Inc., Alabaster, AL) in methanol. The diluted standard solutions of DPPC in the concentration range of 1 to 20 μg/mL were prepared by dilution of the stock standard solution in methanol. The prepared stock standard and diluted standard solutions were injected as calibration standards. The calibration curve for DPPC was fitted to a quadratic function over the concentration range of 1–20 μg/mL with correlation coefficients (R^2) ≥ 0.995. The limit of detection (LOD) and limit of quantitation (LOQ) were 0.31 and 0.94 μg/mL, respectively. The accuracy (as %bias) at concentrations of 5, 10 and 20 μg/mL was ≤7% and precision (as %RSD) was ≤3%. To determine the content uniformity of the Surfactant-EEG powder, approximately 1 mg of the powder was dissolved in 25 mL of methanol and quantitatively analyzed for the DPPC content by the LC-MS method described above. The mean amount of DPPC per mg of Surfactant-EEG formulations was determined. Triplicate samples were prepared and analyzed for each of the powder samples. The loaded drug (DPPC) mass was determined through content uniformity analysis of the Surfactant-EEG powder. The mass of DPPC was also determined from all the deposition sites, and the recovered dose was the total mass recovered from all the deposition sites.

The bulk density of each powder batch was determined using a 1 mL plastic syringe. Briefly, powder mass was calculated as the weight difference between the weight of the empty syringe and the weight of the syringe containing powder. The mass was then divided by the volume occupied by the powder inside the syringe to calculate the powder bulk density. The resulting densities were ~0.10 g/cm^3 for the AS-EEG formulation and ~0.18 g/cm^3 for the Survanta® based Surfactant-EEG formulation.

Statistical Analysis

All experiments were performed with three or more replicates. Statistical analysis was performed using JMP Pro 16 (SAS Institute Inc., Cary, NC). Comparison of air-jet DPI device performance and surfactant formulation sensitivity to flow rate utilized one-way ANOVA followed by post hoc Tukey. Direct comparisons of sensitivity cases utilized Students t-test. Statistical tests used a significance limit of P=0.05.

RESULTS

Comparison of Air-Jet DPI Design

Performance of the four unique PD designs (Figure 2) was initially evaluated using the 10 mg mass loading of the AS-EEG powder formulation. Table I provides the deposition fractions within each region based on the loaded formulation mass, as well as the number of actuations required to provide two consecutive clear actuations (no powder visible exiting the air-jet DPI). PD-2 and PD-3 produced the lowest DPI retention (~11-13%) and the highest tracheal filter deposition of ~60%, which met the goal of achieving 60% estimated lung delivery efficiency. PD-2 and PD-3 also had statistically similar performance across

all deposition regions with the only difference being that PD-2 required one extra actuation to clear the device. PD-4 did not perform as well as the other devices and had the highest variability, based on mean (SD) DPI retention and tracheal filter delivery of 33.2 (5.5) % and 46.2 (2.1) %, respectively. This device also required the highest number of actuations. PD-1 had a mid-range performance with a mean tracheal filter deposition of ~53% and a DPI retention ~17%. PD-1 was also in the mid-range in terms of consistency with larger standard deviations than PD-2 and PD-3, but less than seen with PD-4. Due to the similar and best performance of PD-2 and PD-3, both devices were selected for sensitivity analysis of loaded dose in the next step.

Sensitivity Analysis: Impact of Loaded Dose

To determine if the devices perform similar when loaded with a larger dose of powder, the results of the initial 10 mg powder mass were compared to a 30 mg loaded powder mass of the same formulation. For PD-2 and PD-3, Table II compares the results with 10 mg powder mass loadings from Table I with additional data using 30 mg loadings. For both designs, there was a slight but statistically significant reduction is nasal interface deposition (~2% absolute difference) with the larger loaded dose. PD-3 also produced a slight but statistically significant reduction in the anterior nose deposition region (~1%) with the larger loaded dose. All other regions for both designs remained statistically equivalent, indicating these two designs are not sensitive to the loaded dose for the values tested. It is also observed that the dose delivered on each actuation appears to be consistent. Due to the experimental procedure of delivery, requiring two consecutive visibly clear actuations before ending the trial, it can be inferred that performance will remain similar when PD-2 is actuated 3 and 9 times, and while PD-3 is actuated 2 and 6 times, for a 10 and 30 mg powder mass loading, respectively. For both designs, a 3-fold increase in powder mass also required a 3-fold increase in number of actuations to empty the device, which indicates a similar dose per actuation between the two loaded dose masses. Since both devices performed similarly with the increased loaded dose, only PD-3 was chosen for additional sensitivity analysis in this study to reduce material and time costs of the experiments.

Sensitivity Analysis: Impact of Downstream Pulmonary Mechanics

The second sensitivity analysis utilized the results of PD-3 with a 30 mg powder mass loading of the AS-EEG formulation (from Table II; denoted filter-only), compared to a pulmonary mechanics (PM) outlet condition. All other parameters of the experiment were identical, including number of actuations. The comparison of regional drug deposition for filter-only and PM outlet conditions is presented in Table III. Performance across all deposition regions was statistically similar except for the nasal interface, which decreased by ~1% (absolute difference). The PM outlet condition was not found to have a statistically significant effect on the estimated lung deliver efficiency, which remained about 60%, but demonstrated an increasing trend in lung delivery efficiency (i.e., 60.5% filter only vs. 62.6% PM outlet). Overall, the performance was found to be insensitive to the addition of the PM outlet condition.

Sensitivity Analysis: Impact of Powder Reservoir Volume

The powder reservoir volume sensitivity analysis used the PD-3 device and 10 mg powder mass loading with the AS-EEG formulation. A comparison of the initial results using the standard powder reservoir (Table II data) with additional data using the extended volume powder reservoir is shown in Table IV. The extended volume was not found to have an impact on the deposition found in the nasal interface and nose-throat regions; however, a statistically significant difference was found for the DPI retention (also affecting Total ED) and the tracheal filter. The mean DPI retention increased from 10.9% to 15.5% while the mean tracheal filter deposition decreased from 60.9% to 54.5% with the extended powder reservoir. The nearly 3-fold increase of dead space in the powder reservoir was found to impact the performance of the system by lowering the emitted dose and consequently the tracheal filter deposition by approximately 5% (absolute difference).

Sensitivity Analysis: Impact of Surfactant Formulation

Using the results of the initial PD-3 test with 10 mg of the AS-EEG powder formulation, Figure 7 compares the difference in deposition with the Survanta® based Surfactant-EEG powder formulation under similar conditions. In Figure 7, the total NT deposition represents the sum of the three nose-throat regions of the preterm infant model. A side-by-side comparison is made for the mean deposition fractions within different regions for both formulations, with +/− 1 standard deviation error bars. While the formulation was not found to have a statistically significant effect on device retention, all other regions indicated a statistical difference. Most notable were the differences in Total NT and Filter deposition. Changing from the AS-EEG to the Surfactant-EEG formulation increased the mean Total NT deposition from 23.3% to 47%, and decreased the mean Filter deposition from 60.9% to 30.2%. Due to this significant change in performance, the flow rate was re-evaluated for the Surfactant-EEG formulation as performance has been previously shown to be sensitive to flow rate (17).

Sensitivity Analysis: Impact of Surfactant Formulation Across Different Flow Rates

As a final sensitivity analysis, the effect of flow rate on performance for the Surfactant-EEG formulation was explored, using the two additional Q90 flow rates of 4 and 6 L/min. Figure 8 provides mean deposition fractions across the regions of interest, with +/− 1 standard deviation error bars grouped by flow rate. Statistical analysis using one-way ANOVA ($p<0.05$) showed no significant effect of flow rate on Device retention or Interface deposition, which remained about 11-13% and 3-4%, respectively. The total NT and Filter deposition were, however, found to be affected by the flow rate. Statistical analysis using post-hoc Tukey ($p<0.05$) showed a significant increase in tracheal filter deposition for the 4 L/min case, and a significant increase in NT deposition for the 6 L/min case, when compared to the original 1.7 L/min. The results of the flow rate sensitivity analysis for the Surfactant-EEG powder formulation demonstrated best performance at a Q90 of 4 L/min, which improved the mean estimated lung delivery efficiency to 38.6%.

DISCUSSION

A significant outcome of this study is the advancement of the infant air-jet DPI system to enable high dose powder loadings using a passive cyclic loading approach. Four new passive design (PD) devices were implemented and two of the designs (PD-2 and PD-3) resulted in improved estimated lung delivery efficiencies over the previously developed system (e.g., Howe et al. (17) with ~50% lung delivery efficiency), while also enabling high dose delivery. Both PD-2 and PD-3 performed similarly when loaded with a 10 and 30 mg mass of AS-EEG formulation, and were able to deliver ~60% of the loaded dose to the tracheal filter through a preterm NT model. Based on the observation that tripling the loaded dose did not have an impact on lung delivery efficiency, it is projected that mass loadings can be increased even further without negative impacts. Furthermore, tripling the volume of the powder reservoir resulted in only a minor reduction in lung delivery efficiency from ~60% to ~55%. As a result, the passive cyclic loading strategy appears capable of delivering a range of drug masses from ~10 mg through ~150 mg (at a powder bulk density of 0.1 g/cm^3) with only minor changes in lung delivery efficiency. Including downstream pulmonary mechanics consistent with a preterm infant was also observed to produce a negligible impact on platform performance and lung delivery efficiency of the aerosol. Considered collectively, results of this study indicate that the infant air-jet DPI expanded with passive cyclic loading is expected to exhibit consistent performance across a range of loaded doses and is largely insensitive to pulmonary mechanics.

In contrast with loaded dose, reservoir volume size and downstream conditions, performance of the infant air-jet DPI was found to be sensitive to characteristics of the loaded formulation, as expected. While the platform using the PD-3 device was able to achieve 60% lung delivery efficiency with the AS-EEG formulations, performance was significantly different when delivering the Surfactant-EEG powder. The powder formulations had similar primary particle size characteristics with Dv50's of 1.24 and 1.14 μm for the Surfactant-EEG and AS-EEG formulations, respectively, when measured using laser diffraction (Symptec HELOS with RODOS/M disperser at 4 bar; Sympatec GmbH, Clausthal-Zellerfeld, Germany). However, the Surfactant-EEG formulation produced a ~2-fold increase in total NT deposition as well as an equivalent decrease in tracheal filter deposition, at the 1.7 L/min flow rate. Differences in powder dispersion properties are likely the driving cause for the change in performance, and increasing the flow rate provides a means to provide additional energy to better deaggregate the formulation and produce the aerosol. As mentioned in our previous study (17), the optimal flow rate is likely to be device and formulation dependent, and therefore an additional sensitivity analysis was performed for the PD-3 device and the Surfactant-EEG formulation. Lung delivery performance was found to improve when increasing the flow rate to 4 L/min, and then fall when further increased to 6 L/min, likely due to additional turbulence and impaction aerosol losses in the interface and NT airways. Out of the three flow rates tested, the estimated lung delivery efficiency for Surfactant-EEG peaked at nearly 40% with the 4 L/min flow rate; however, NT deposition remained high, between 40-50%.

Additional ways to improve performance with the Surfactant-EEG formulation include the use of a mesh interface or adjusting the shelf height in the aerosolization chamber. Previous

investigation on nasal interface design has shown that using a metal mesh incorporated into the nasal interface can significantly reduce NT deposition (18). With the high NT deposition found with the Surfactant-EEG formulation, inclusion of a mesh may significantly improve performance. Furthermore, the shelf inside the aerosolization chamber of PD-2 and PD-3 has been optimized for the AS-EEG formulation. For example, the shelf in the PD-2 device is positioned such that ~2.6 mg of the AS-EEG powder can fall and rest on the shelf for each actuation. Compared to the density of the AS-EEG powder (~0.10 g/cm^3), the Survanta® based Surfactant-EEG powder was more dense, at approximately 0.18 g/cm^3, resulting in ~4.7 mg of powder resting on the shelf between actuations, which may diminish aerosolization or create cloud motion phenomenon, which increases the deposition of all elements in the cloud (41, 42). Adjusting the shelf spacing for each formulation and respective density may prove beneficial.

Limitations of this study include the use of a single preterm NT model, a single nasal interface, and limited number of devices. The use of a single preterm NT airway geometry limits the deposition data to a single point; however, in a previous study investigating nasal interfaces (18), the performance of the infant air-jet platform remained statistically similar across two preterm NT models with very different airway features. Also guided by the previous nasal interface study (18), only a single nasal interface was used in this study, whereas the inclusion of a mesh based design may improve results, specifically for the Surfactant-EEG formulation. Finally, with only 4 unique passive cyclic loading air-jet DPI designs, the range of performance this selection captures is unknown. However, for the devices tested in this study, especially PD-2 and PD-3, the performance meets the initially established lung delivery efficiency goal of 60% with the AS-EEG formulation. Additional testing and modification will need to be explored for other formulations to further improve lung delivery efficiency. While it is anticipated that lung delivery performance will remain relatively unchanged up to dose loadings of 150 mg at a powder bulk density of 0.1 g/cm^3, this evaluation was not performed in this study.

Considering the example of surfactant replacement therapy using the Survanta® based Surfactant-EEG formulation, Kamga Gninzeko (43) evaluated efficacy in an animal model of surfactant depleted rats. Significant improvements in rat pulmonary mechanics were observed with the Surfactant-EEG formulation at a phospholipid (PL) dose of 1.5 mg per kg of animal body weight. Assuming that 1.5 mg/kg of PL will be effective in a human infant, the required Surfactant-EEG powder mass for a body weight of 1.6 kg would be ~20 mg, factoring in 25% PL loading in the formulation and a 50% lung delivery efficiency. Assuming the same conditions, the powder mass loading for a full-term infant with a weight of 3.55 kg would be ~44 mg. Based on the results of this study, the infant air-jet DPI with passive cyclic loading appears capable of delivering this range of powder dose with minimal expected change in lung delivery performance. Other recent studies on the use of aerosol surfactant replacement therapy in animal models have indicated much higher required doses for positive efficacy, in the range of 100 to 240 mg/kg (44-46) and higher (47-49). Through the use of an expanded powder reservoir, it appears that the passive cyclic loading approach could also be used to deliver powder versions of these much higher doses with a single loading of the device and potentially at a controlled rate.

CONCLUSIONS

In conclusion, a passive cyclic loading approach was successfully implemented for the infant air-jet DPI platform. During *in vitro* testing using a preterm NT model and AS-EEG formulation, the platform performed consistently when the loaded dose increased from 10 mg to 30 mg and also when connected to the pulmonary mechanics outlet condition. The optimal PD devices (PD-2 and PD-3) achieved an estimated lung delivery efficiency of ~60% when administered through a 1600 g preterm NT model. The performance was notably different when the Surfactant-EEG powder was used, which led to an increase in NT deposition and decrease in tracheal filter deposition. It is likely adjustments to the aerosolization chamber and passive cyclic loading system will be needed for each new formulation. In this study, modifying the flow rate alone produced an increased estimated lung delivery efficiency from 30% to nearly 40% at flow rates of 1.7 and 4.0 L/min, respectively. Additional modifications will likely further improve performance when using a Surfactant-EEG formulation. Further optimization of the platform with passive cyclic loading will allow for a highly efficient, rapid, and non-invasive form of aerosol delivery to neonates with selectable dosage and expected consistent performance.

FUNDING INFORMATION

Research reported in this publication was supported by the Eunice Kennedy Shriver National Institute of Child Health & Human Development of the National Institutes of Health under Award Number R01HD087339 and by the National Heart, Lung and Blood Institute of the National Institutes of Health under Award Number R01HL139673. The content is solely the responsibility of the authors and does not necessarily represent the official views of the National Institutes of Health.

References

1. Willson DF. Aerosolized surfactants, anti-inflammatory drugs, and analgesics. Respiratory Care. 2015;60:774–793. [PubMed: 26070574]
2. DiBlasi RM. Clinical controversies in aerosol therapy for infants and children. Respiratory Care. 2015;60:894–916. [PubMed: 26070582]
3. Everard ML. Inhaler devices in infants and children: Challenges and solutions. Journal of Aerosol Medicine-Deposition Clearance and Effects in the Lung. 2004;17:186–195.
4. Fink JB. Aerosol delivery to ventilated infant and pediatric patients. Respiratory Care. 2004;49:653–665. [PubMed: 15165300]
5. Fink JB. Delivery of inhaled drugs for infants and small children: a commentary on present and future needs. Clinical Therapeutics. 2012;34:S36–S45. [PubMed: 23149011]
6. Fok TF, Monkman S, Dolovich M, Gray S, Coates G, Paes B, Rashid F, Newhouse M, and Kirpalani H. Efficiency of aerosol medication delivery from a metered dose inhaler versus jet nebulizer in infants with bronchopulmonary dysplasia. Pediatric Pulmonology. 1996;21:301–309. [PubMed: 8726155]
7. Corcoran TE, Saville A, Adams PS, Johnston DJ, Czachowski MR, Domnina YA, Lin JH, Weiner DJ, Huber AS, and Sanchez De Toledo J. Deposition studies of aerosol delivery by nasal cannula to infants. Pediatric Pulmonology. 2019;54:1319–1325. [PubMed: 30932345]
8. Nord A, Linner R, Salomone F, Bianco F, Ricci F, Murgia X, Schlun M, Cunha-Goncalves D, and Perez-de-Sa V. Lung deposition of nebulized surfactant in newborn piglets: Nasal CPAP vs Nasal IPPV. Pediatric Pulmonology. 2019;
9. Sunbul FS, Fink JB, Harwood R, Sheard MM, Zimmerman RD, and Ari A. Comparison of HFNC, bubble CPAP and SiPAP on aerosol delivery in neonates: An in-vitro study. Pediatric Pulmonology. 2015;50:1099–1106. [PubMed: 25491434]

10. El Taoum KK, Xi J, Kim J, and Berlinski A. In vitro evaluation of aerosols delivered via the nasal route. Respiratory Care. 2015;60:1015–1025. [PubMed: 25587167]
11. Réminiac F, Vecellio L, Loughlin RM, Le Pennec D, Cabrera M, Vourc'h NH, Fink JB, and Ehrmann S. Nasal high flow nebulization in infants and toddlers: an in vitro and in vivo scintigraphic study. Pediatric Pulmonology. 2017;52:337–344. [PubMed: 27392199]
12. Fok TF, Alessa M, Monkman S, Dolovich M, Girard L, Coates G, and Kirpalani H. Pulmonary deposition of salbutamol aerosol delivered by metered dose inhaler, jet nebulizer, and ultrasonic nebulizer in mechanically ventilated rabbits. Pediatric Research. 1997;42:721–727. [PubMed: 9357949]
13. Amirav I, Balanov I, Gorenberg M, Luder AS, Newhouse MT, and Groshar D. Beta-agonist aerosol distribution in respiratory syncytial virus bronchiolitis in infants. Journal of Nuclear Medicine. 2002;43:487–491. [PubMed: 11937592]
14. Mallol J, Rattray S, Walker G, Cook D, and Robertson CF. Aerosol deposition in infants with cystic fibrosis. Pediatric Pulmonology. 1996;21:276–281. [PubMed: 8726152]
15. Chua H, Collis G, Newbury A, Chan K, Bower G, Sly P, and Le Souef P. The influence of age on aerosol deposition in children with cystic fibrosis. European Respiratory Journal. 1994;7:2185–2191. [PubMed: 7713202]
16. Howe C, Hindle M, Bonasera S, Rani V, and Longest PW. Initial Development of an Air-Jet Dry Powder Inhaler for Rapid Delivery of Pharmaceutical Aerosols to Infants. Journal of Aerosol Medicine and Pulmonary Drug Delivery. 2021;34:57–70. [PubMed: 32758026]
17. Howe C, Momin MA, Farkas DR, Bonasera S, Hindle M, and Longest P. Advancement of the Infant Air-Jet Dry Powder Inhaler (DPI): Evaluation of Different Positive-Pressure Air Sources and Flow Rates. Pharmaceutical Research. 2021;38:1615–1632. [PubMed: 34462876]
18. Howe C, Momin MA, Bass K, Aladwani G, Bonasera S, Hindle M, and Longest PW. In Vitro Analysis of Nasal Interface Options for High-Efficiency Aerosol Administration to Preterm Infants. Journal of Aerosol Medicine and Pulmonary Drug Delivery. 2022;10.1089/jamp.2021.0057
19. Boc S, Momin MA, Farkas DR, Longest W, and Hindle M. Performance of Low Air Volume Dry Powder Inhalers (LV-DPI) when Aerosolizing Excipient Enhanced Growth (EEG) Surfactant Powder Formulations. AAPS PharmSciTech. 2021;22:1–12.
20. Boc S, Momin MA, Farkas DR, Longest W, and Hindle M. Development and Characterization of Excipient Enhanced Growth (EEG) Surfactant Powder Formulations for Treating Neonatal Respiratory Distress Syndrome. AAPS PharmSciTech. 2021;22:1–12.
21. Weers J. Inhaled antimicrobial therapy - Barriers to effective treatment. Advanced Drug Delivery Reviews. 2015;85:24–43. [PubMed: 25193067]
22. Walsh BK, Betit P, Fink JB, Pereira LM, and Arnold J. Characterization of ribavirin aerosol with small particle aerosol generator and vibrating mesh micropump aerosol technologies. Respiratory Care. 2016;61:577–585. [PubMed: 26932383]
23. Wright M, Mullett CJ, and Piedimonte G. Pharmacological management of acute bronchiolitis. Therapeutics and Clinical Risk Management. 2008;4:895. [PubMed: 19209271]
24. Farkas D, Hindle M, and Longest PW. Application of an inline dry powder inhaler to deliver high dose pharmaceutical aerosols during low flow nasal cannula therapy. International Journal of Pharmaceutics. 2018;546:1–9. [PubMed: 29733972]
25. Farkas DR, Hindle M, and Longest PW. Characterization of a new high-dose dry powder inhaler (DPI) based on a fluidized bed design. Annals of Biomedical Engineering. 2015;43:2804–2815. [PubMed: 25986955]
26. Young PM, Crapper J, Philips G, Sharma K, Chan H-K, and Traini D. Overcoming dose limitations using the Orbital multi-breath dry powder inhaler. Journal of Aerosol Medicine and Pulmonary Drug Delivery. 2013;DOI: 10.1089/jamp.2013.1080
27. Yeung S, Traini D, Tweedie A, Lewis D, Church T, and Young PM. Assessing aerosol performance of a dry powder carrier formulation with increasing doses using a novel inhaler. AAPS PharmSciTech. 2019;20:1–12.

28. Geller DE, Weers J, and Heuerding S. Development of an inhaled dry-powder formulation of Tobramycin using PulmoSphereTM technology. Journal of Aerosol Medicine and Pulmonary Drug Delivery. 2011;24:175–182. [PubMed: 21395432]
29. Bilton D, Robinson P, Cooper P, Gallagher CG, Kolbe J, Fox H, Jaques A, and Charlton B. Inhaled dry powder mannitol in cystic fibrosis: an efficacy and safety study. European Respiratory Journal. 2011;38:1071–1080. [PubMed: 21478216]
30. Smith IJ, Bell J, Bowman N, Everard M, Stein S, and Weers JG. Inhaler Devices: What Remains to be Done? Journal Of Aerosol Medicine And Pulmonary Drug Delivery. 2010;23:S25–S37. [PubMed: 21133798]
31. Son Y-J, Longest PW, and Hindle M. Aerosolization characteristics of dry powder inhaler formulations for the excipient enhanced growth (EEG) application: Effect of spray drying process conditions on aerosol performance. International Journal of Pharmaceutics. 2013;443:137–145. [PubMed: 23313343]
32. Boc ST, Farkas DR, Longest PW, and Hindle M. Spray dried pulmonary surfactant powder formulations: Development and characterization. Respiratory Drug Delivery 2018. 2018;2:635–638.
33. Bass K, Boc S, Hindle M, Dodson K, and Longest W. High-Efficiency Nose-to-Lung Aerosol Delivery in an Infant: Development of a Validated Computational Fluid Dynamics Method. Journal of Aerosol Medicine and Pulmonary Drug Delivery. 2019;32:132–148. [PubMed: 30556777]
34. Fenton. Fenton Preterm Growth Charts. https://live-ucalgary.ucalgary.ca/resource/preterm-growth-chart/preterm-growth-chart. 2013;
35. Dave MH, Kemper M, Schmidt AR, Both CP, and Weiss M. Pediatric airway dimensions—A summary and presentation of existing data. Pediatric Anesthesia. 2019;29:782–789. [PubMed: 31087466]
36. Bhutani VK, Bowen FW, and Sivieri EM. Postnatal changes in pulmonary mechanics and energetics of infants with respiratory distress syndrome following surfactant treatment. Neonatology. 2005;87:323–331.
37. Snepvangers Y, de Winter JP, Burger H, Brouwers H, and van der Ent CK. Respiratory outcome in preterm ventilated infants: importance of early respiratory system resistance. European Journal of Pediatrics. 2004;163:378–384. [PubMed: 15107987]
38. Choukroun M, Tayara N, Fayon M, and Demarquez J. Early respiratory system mechanics and the prediction of chronic lung disease in ventilated preterm neonates requiring surfactant treatment. Neonatology. 2003;83:30–35.
39. Volsko TA, Fedor K, Amadei J, and Chatburn RL. High flow through a nasal cannula and CPAP effect in a simulated infant model. Respiratory Care. 2011;56:1893–1900. [PubMed: 21682982]
40. Li D, Xiong X, Bai Q, Yang W, Zhao R, and Zhang A. Development and validation of an LC-MS/MS method for quantification of dipalmitoylphosphatidylcholine as a promising biomarker for renal failure in urine. Journal of Chinese Pharmaceutical Sciences. 2015;24:73–79.
41. Kolanjiyil AV, Hosseini S, Alfaifi A, Farkas D, Walenga R, Babiskin A, Hindle M, Golshahi L, and Longest PW. Validating CFD predictions of nasal spray deposition: Inclusion of cloud motion effects for two spray pump designs. Aerosol Science and Technology. 2022;56:305–322.
42. Kolanjiyil AV, Hosseini S, Alfaifi A, Hindle M, Golshahi L, and Longest PW. Importance of cloud motion and two-way momentum coupling in the transport of pharmaceutical nasal sprays. Journal of Aerosol Science. 2021;156:105770.
43. Kamga Gninzeko FJ, Valentine MS, Tho CK, Chindal SR, Boc S, Dhapare S, Momin MAM, Hassan A, Hindle M, and Farkas DR. Excipient Enhanced Growth Aerosol Surfactant Replacement Therapy in an In Vivo Rat Lung Injury Model. Journal of Aerosol Medicine and Pulmonary Drug Delivery. 2020;33:314–322. [PubMed: 32453638]
44. Walther FJ, Hernández-Juviel JM, and Waring AJ. Aerosol delivery of synthetic lung surfactant. PeerJ. 2014;2:e403. [PubMed: 24918030]
45. Walther FJ, Waring AJ, Otieno M, and DiBlasi RM. Efficacy, dose–response, and aerosol delivery of dry powder synthetic lung surfactant treatment in surfactant-deficient rabbits and premature lambs. Respiratory Research. 2022;23:1–16. [PubMed: 34983515]

46. Walther FJ, Gupta M, Lipp MM, Chan H, Krzewick J, Gordon LM, and Waring AJ. Aerosol delivery of dry powder synthetic lung surfactant to surfactant-deficient rabbits and preterm lambs on non-invasive respiratory support. Gates Open Research. 2019;3

47. Ruppert C, Kuchenbuch T, Boensch M, Schmidt S, Mathes U, Hillebrand V, Henneke I, Markart P, Reiss I, Schermuly RT, Seeger W, and Gunther A. Dry powder aerosolization of a recombinant surfactant protein-C-based surfactant for inhalative treatment of the acutely inflamed lung. Critical Care Medicine. 2010;38:1584–1591. [PubMed: 20400897]

48. Hutten MC, Kuypers E, Ophelders DR, Nikiforou M, Jellema RK, Niemarkt HJ, Fuchs C, Tservistas M, Razetti R, and Bianco F. Nebulization of Poractant alfa via a vibrating membrane nebulizer in spontaneously breathing preterm lambs with binasal continuous positive pressure ventilation. Pediatric Research. 2015;78:664–669. [PubMed: 26322413]

49. Bianco F, Ricci F, Catozzi C, Murgia X, Schlun M, Bucholski A, Hetzer U, Bonelli S, Lombardini M, and Pasini E. From bench to bedside: in vitro and in vivo evaluation of a neonate-focused nebulized surfactant delivery strategy. Respiratory Research. 2019;20:134. [PubMed: 31266508]

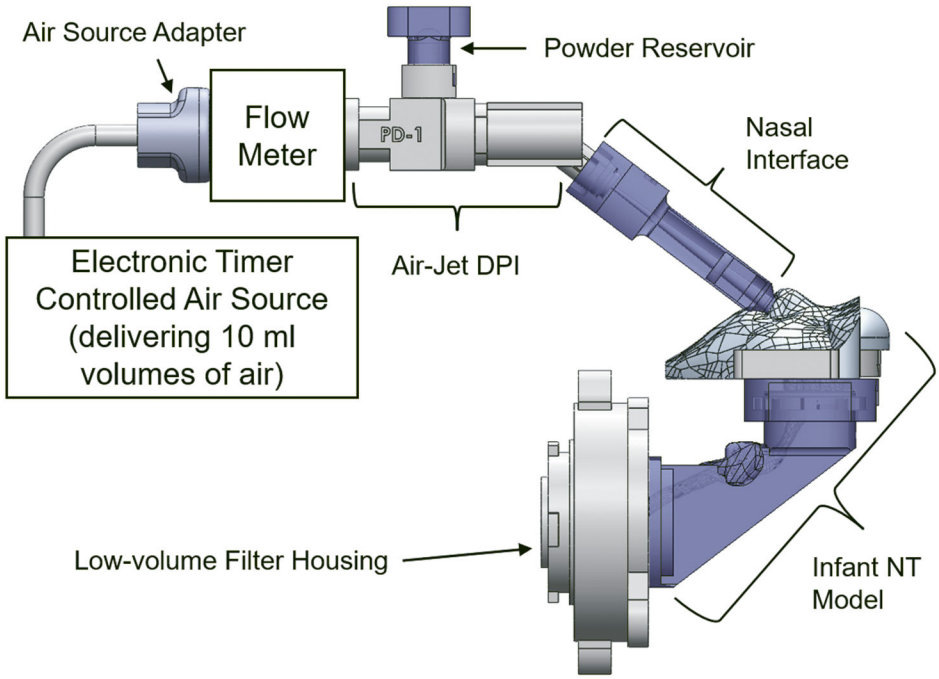

Fig. 1.

Graphical overview of the experimental setup including the infant air-jet DPI platform with passive cyclic loading

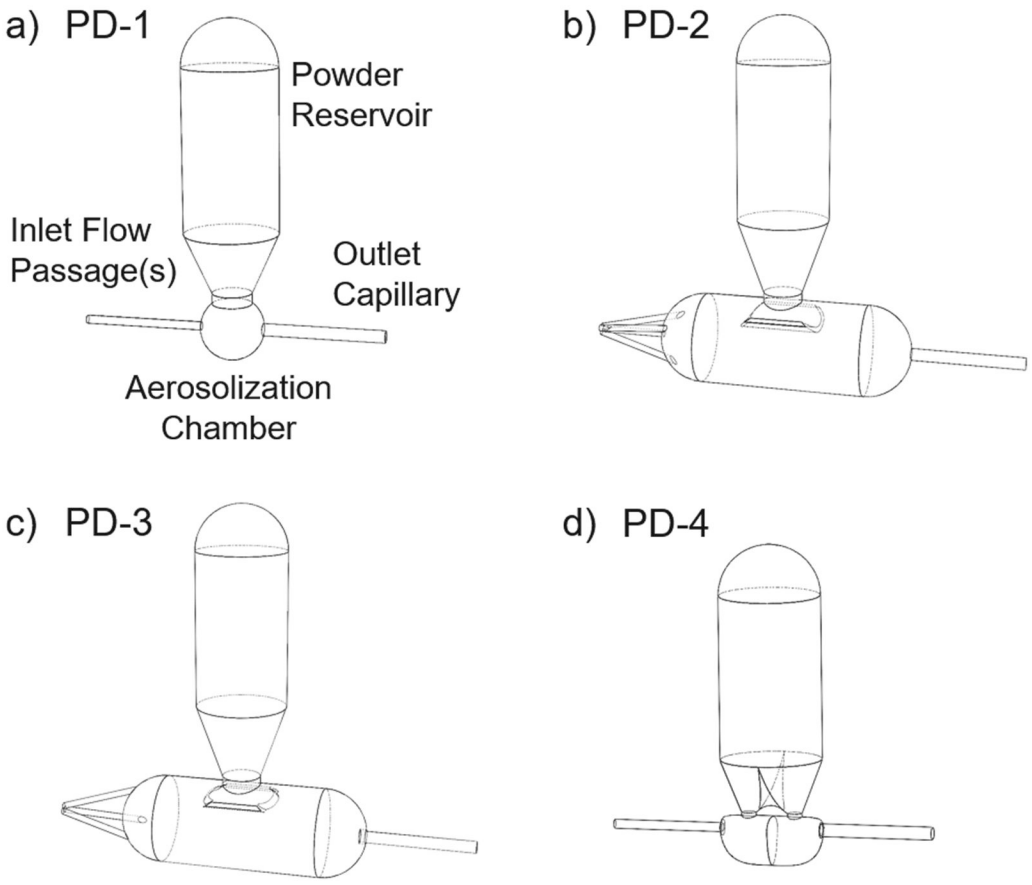

Fig. 2.

Internal airflow geometry of each infant air-jet DPI passive design (PD) from air source inlet (left side of each image) to the device outlet (right side of each image). Panels **(a)-(d)** correspond to PD-1, PD-2, PD-3, and PD-4, respectively

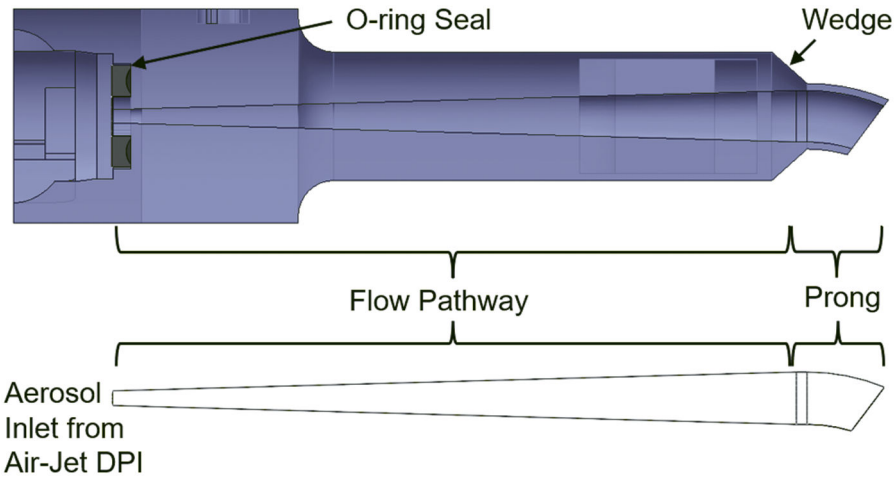

Fig. 3.

Overview of the single nasal interface used in this study illustrating the flow pathway and prong regions. A cross sectional view rendering (above) depicts interface features including O-ring seal and exterior prong wedge, while the internal airway geometry is pictured below. The nasal prong employed a short curve and was produced in rigid material

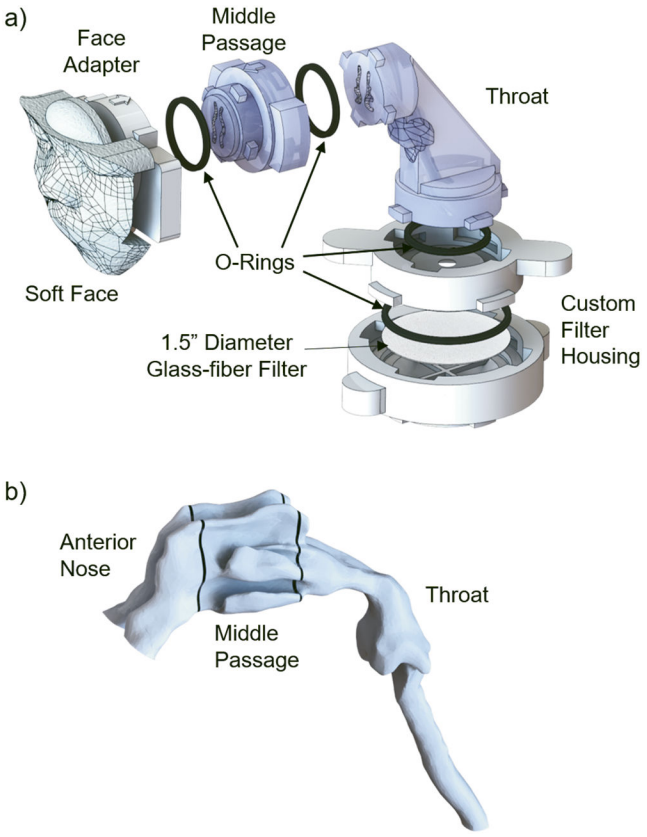

Fig. 4.

Schematic overview of the preterm infant NT airway model and regional sections. **(a)** Assembly of infant NT model with connection to custom low-volume filter housing with parts labeled (the Soft Face and Face Adapter segments are glued together before use and represent the Anterior Nose airway region). **(b)** Internal airway geometry of the infant NT model with assessed regions including the anterior nose, middle passage and throat.

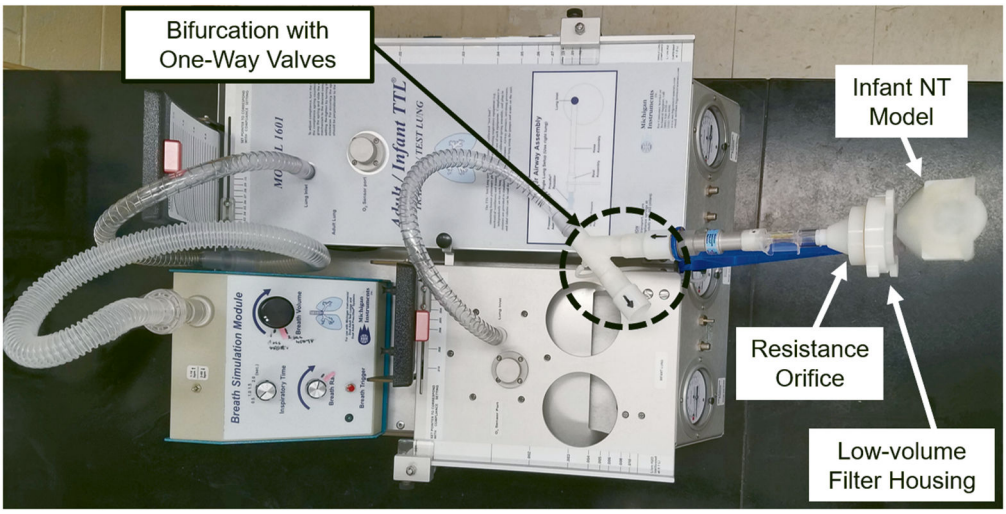

Fig. 5.

Experimental setup for sensitivity analysis testing with the infant NT model connected to the infant pulmonary mechanics (PM) outlet condition and breathing simulator. All custom components are labeled

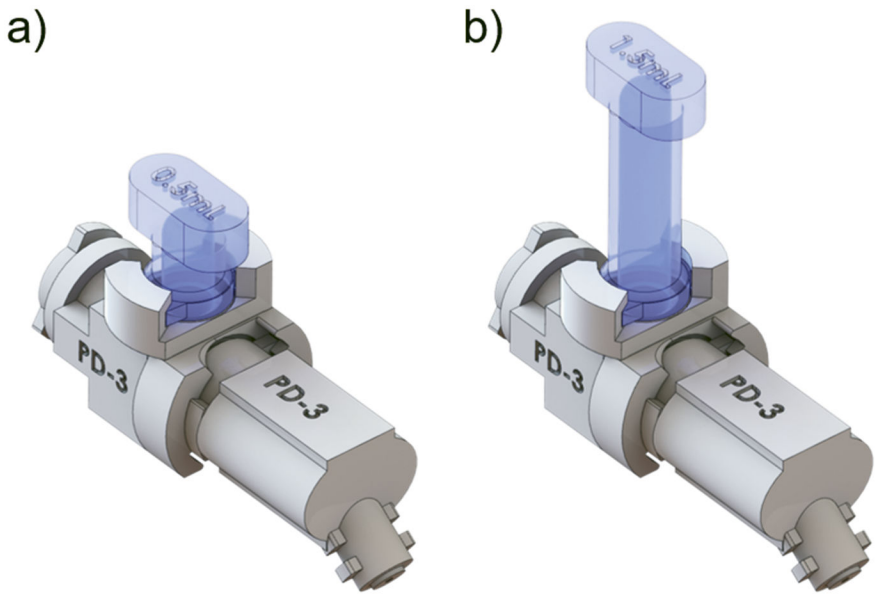

Fig. 6.

Renderings of the two device configurations for the powder reservoir sensitivity analysis. **(a)** PD-3 device with standard (0.55 mL) volume reservoir attached and **(b)** PD-3 device with extended (1.5 mL) volume reservoir attached

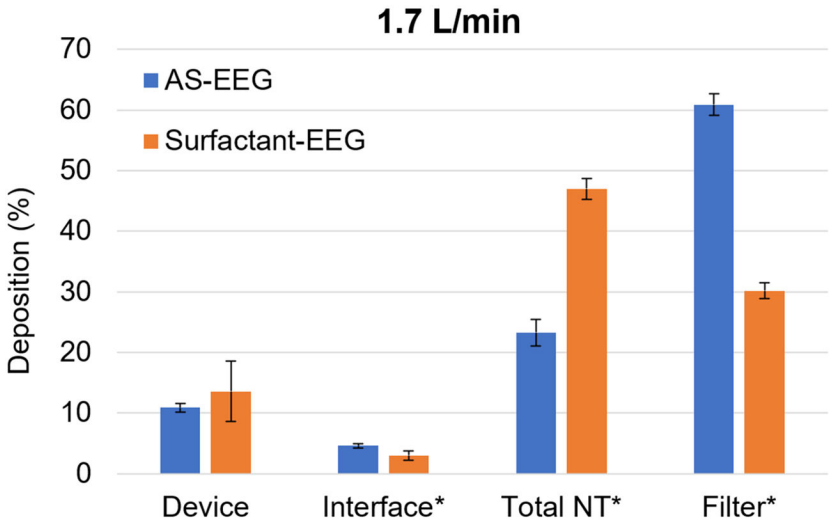

Fig. 7.

Plot of experimentally determined mean (SD) drug deposition fractions (based on loaded dose) of the AS-EEG formulation compared with the Surfactant-EEG formulation grouped by deposition region, at a Q90 flow rate of 1.7 L/min [n=3]. Anterior nose, middle passage (MP), and throat deposition fractions were summed to form the total NT deposition. Significant effect ($p<0.05$) of formulation found in the interface, total NT, and filter deposition regions (t-test)

*$p<0.05$ significant effect of formulation on deposition region (t-test).

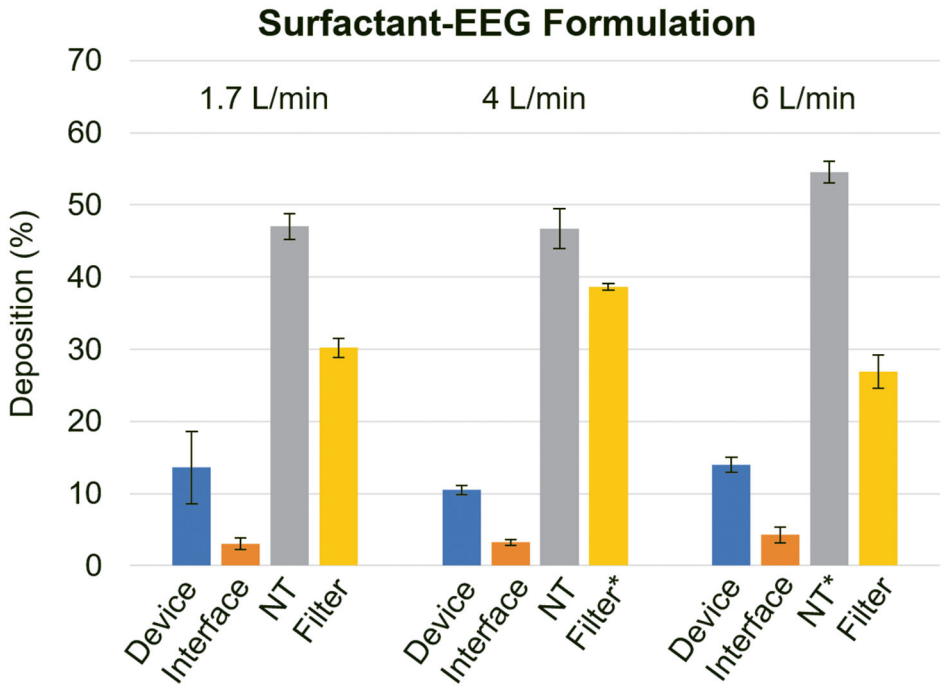

Fig. 8.

Experimentally determined mean (SD) drug deposition fractions (based on loaded dose) of the Surfactant-EEG formulation for different Q90 flow rates [n=3]. Anterior nose, middle passage (MP), and throat deposition fractions were summed to form the total NT deposition. Significant difference ($p<0.05$) found for filter deposition at 4 L/min and for NT at 6 L/min when compared to the original 1.7 L/min case (one-way ANOVA followed by post-hoc Tukey)

*$p<0.05$ significant difference compared with 1.7 L/min flow rate (one-way ANOVA followed by post-hoc Tukey).

Table I:

Lung delivery efficiencies (estimated as Tracheal Filter %) and regional deposition fractions (based on 10 mg loaded dose) for the AS-EEG formulation and an initial round of different device designs.

	PD-1	PD-2	PD-3	PD-4
# of Actuations	4	5	4	6
Deposition Region				
DPI Retention (%)[a]	16.8 (4.8)	12.9 (1.1)	10.9 (0.7)	33.2 (5.5)[b]
Nasal Interface (%)	5.2 (0.4)	4.3 (0.2)	4.6 (0.3)	4.0 (1.1)
Total ED (%)[a]	77.9 (4.6)	82.8 (1.2)	84.5 (0.4)	62.8 (5.5)[b]
Anterior Nose (%)	4.8 (1.0)	5.4 (1.6)	4.5 (0.3)	3.2 (1.1)
Middle Passage (%)[a]	7.8 (0.9)	7.8 (0.4)	8.4 (1.4)	5.0 (1.3)[b]
Throat (%)	11.5 (3.1)	9.1 (0.9)	10.4 (1.3)	6.3 (4.6)
Total NT (%)	24.1 (4.9)	22.3 (1.1)	23.2 (2.1)	14.4 (7.0)
Tracheal Filter (%)[a]	53.1 (1.7)	60.0 (0.6)[b]	60.9 (1.9)[b]	46.2 (2.1)[b]

Mean values with standard deviations (SD) shown in parenthesis, n=3.

[a] $p<0.05$ significant effect of design on deposition region (one-way ANOVA).

[b] $p<0.05$ significant difference compared to PD-1 case (post-hoc Tukey).

DPI, dry powder inhaler; ED, emitted dose; NT, nose-throat; PD, passive design.

Table II:

Lung delivery efficiencies (estimated as Tracheal Filter %) and regional deposition fractions (based on loaded dose) for the AS-EEG formulation and comparisons of 10 vs 30 mg loaded powder in lead devices.

	PD-2		PD-3	
	10mg	**30mg**	**10mg**	**30mg**
# of Actuations	5	11	4	8
Deposition Region				
DPI Retention (%)	12.9 (1.1)	16.1 (2.1)	10.9 (0.7)	12.2 (2.9)
Nasal Interface (%)	4.3 (0.2)	2.4 (0.1)[a]	4.6 (0.3)	2.8 (0.4)[a]
Total ED (%)	82.8 (1.2)	81.5 (2.0)	84.5 (0.4)	85.0 (3.3)
Anterior Nose (%)	5.4 (1.6)	3.3 (0.3)	4.5 (0.3)	3.7 (0.5)[a]
Middle Passage (%)	7.8 (0.4)	8.2 (0.3)	8.4 (1.4)	8.3 (0.5)
Throat (%)	9.1 (0.9)	10.6 (0.9)	10.4 (1.3)	12.3 (1.3)
Total NT (%)	22.3 (1.1)	22.1 (1.0)	23.2 (2.1)	24.4 (1.3)
Tracheal Filter (%)	60.0 (0.6)	58.5 (1.3)	60.9 (1.9)	60.5 (1.6)

Mean values with standard deviations (SD) shown in parenthesis, n=3.

[a] $p<0.05$ significant difference in deposition region compared with 10 mg case (t-test).

Table III:

Lung delivery efficiencies (estimated as Tracheal Filter %) and regional deposition fractions (based on loaded dose) of the AS-EEG formulation and 30 mg dose loadings with the PD-3 device and filter-only vs. pulmonary mechanics (PM) outlet conditions.

Deposition Region	Filter-Only	PM
DPI Retention (%)	12.2 (2.9)	10.5 (1.1)
Nasal Interface (%)	2.8 (0.4)	1.7 (0.5)[a]
Total ED (%)	85.0 (3.3)	87.8 (1.4)
Anterior Nose (%)	3.7 (0.5)	3.7 (0.4)
Middle Passage (%)	8.3 (0.5)	7.9 (0.9)
Throat (%)	12.3 (1.3)	12.3 (0.7)
Total NT (%)	24.4 (1.3)	23.9 (0.7)
Tracheal Filter (%)	60.5 (1.6)	62.6 (1.4)

Mean values with standard deviations (SD) shown in parenthesis, n=3.

[a] $p<0.05$ significant difference between filter-only and PM outlet condition for nasal interface deposition (t-test).

PM, pulmonary mechanics

Table IV:

Lung delivery efficiencies (estimated as Tracheal Filter %) and regional deposition fractions (based on loaded dose) for the AS-EEG formulation and comparisons of standard (0.55 mL) vs extended (1.5 mL) powder reservoir volume with the PD-3 device.

Deposition Region	Standard	Extended
DPI Retention (%)	10.9 (0.7)	15.5 (0.9)[a]
Nasal Interface (%)	4.6 (0.3)	4.5 (0.3)
Total ED (%)	84.5 (0.4)	79.9 (1.1)[a]
Anterior Nose (%)	4.5 (0.3)	4.9 (0.8)
Middle Passage (%)	8.4 (1.4)	9.6 (0.2)
Throat (%)	10.4 (1.3)	11.1 (0.8)
Total NT (%)	23.2 (2.1)	25.6 (1.0)
Tracheal Filter (%)	60.9 (1.9)	54.5 (2.3)[a]

Mean values with standard deviations (SD) shown in parenthesis, n=3.

[a] $p<0.05$ significant difference between standard and extended chamber volume (t-test).